



**HAL**  
open science

## A Delivery System for Precursor Vapors Based on Sublimation in a Fluidized Bed.

Constantin Vahlas, Brigitte Caussat, François Senocq, Wayne L. Gladfelter, Lyacine Aloui, Tyler Moersch

► **To cite this version:**

Constantin Vahlas, Brigitte Caussat, François Senocq, Wayne L. Gladfelter, Lyacine Aloui, et al.. A Delivery System for Precursor Vapors Based on Sublimation in a Fluidized Bed.. Chemical Vapor Deposition, 2007, 1 (2-3), pp.123-129. 10.1002/cvde.200606513 . hal-03481298

**HAL Id: hal-03481298**

**<https://hal.science/hal-03481298>**

Submitted on 15 Dec 2021

**HAL** is a multi-disciplinary open access archive for the deposit and dissemination of scientific research documents, whether they are published or not. The documents may come from teaching and research institutions in France or abroad, or from public or private research centers.

L'archive ouverte pluridisciplinaire **HAL**, est destinée au dépôt et à la diffusion de documents scientifiques de niveau recherche, publiés ou non, émanant des établissements d'enseignement et de recherche français ou étrangers, des laboratoires publics ou privés.

DOI: 10.1002/cvde.200606513

## Full Paper

## A Delivery System for Precursor Vapors Based on Sublimation in a Fluidized Bed\*\*

By Constantin Vahlas,\* Brigitte Caussat, François Senocq, Wayne L. Gladfelter, Lyacine Aloui, and Tyler Moersch

A fluidized-bed, solid-precursor delivery system is found to overcome the mass and heat transport problems encountered in a fixed-bed system. To achieve ideal fluidization behavior, a combination of solid precursor (minor component) and inert particles such as alumina or silica (major component) are charged to the vessel. Using  $[\text{Al}(\text{acac})_3]$  as a test precursor and operating at 423K, the rate of mass transport is measured as a function of the carrier gas flow rate. When operating at carrier gas flow rates above the minimum value required to fluidize the bed, the precursor flow rate significantly exceeds the performance of the fixed-bed system. A simple model of a solid-precursor delivery system is developed to quantify the relationship between operating conditions and gas-phase precursor flow rate. The concept of the fluidized bed, solid-precursor delivery system is validated by directing the precursor and carrier gas mixture into a CVD reactor where the flow is combined with a source of water vapor and oxygen to deposit amorphous  $\text{Al}_2\text{O}_3$  films on coupons of a Ti6242 alloy.

Keywords: Aluminum acetylacetonate, Fluidization, Precursors, Sublimation, Vapors

## 1. Introduction

In most industrial CVD processes, the molecular precursor is a gas (e.g.,  $\text{SiH}_4$ ) or a liquid (e.g.,  $\text{GaMe}_3$ ) at room temperature. Recent attempts to improve CVD processes by designing new precursors have encountered a common problem. As the size and complexity of the molecular precursor are increased, the state of the precursor at standard temperature and pressure becomes a solid.

Three primary problems occur with solid precursors. First, the equilibrium vapor pressure of most solids of interest for CVD is relatively low (typically below 200 Pa at room temperature) compared to liquids. This problem is compounded by the fact that it is often difficult to saturate the carrier gas with the precursor. Raising the temperature of the precursor vessel increases the gas-phase precursor

concentration, but this requires that all lines and valves in contact with the carrier gas flow be heated and can lead to precursor degradation. The second common problem is maintaining a reproducible precursor vapor pressure. During the course of a single run, especially if it is lengthy, the gas-phase precursor concentration may decrease with time. From run to run similar changes are often observed. The instability of the precursor delivery rate with time is caused by changes in the particle size that affect the total surface area. Local variations in temperature can alter the precursor vapor pressure. Finally, particle contamination is possible if suitable safeguards are not built into the precursor delivery line.

A number of alternative, solid-precursor delivery methods have been published or patented. The simplest approach is to raise the precursor vessel temperature above the melting point of the solid. The precursor,  $\text{Me}_3\text{P-InMe}_3$ , used in InP metal-organic (MO) CVD melts at 313K and is used as a liquid precursor.<sup>[1]</sup> A large number of publications and several commercial liquid delivery systems have appeared.<sup>[2-5]</sup> In these systems the solid precursor is dissolved in a compatible solvent that is transported into a heated chamber where both the solvent and the precursor are rapidly vaporized. The design of the heated chamber varies, but the goal is to minimize the time that the precursor spends at the elevated temperature. Ideally, one seeks to vaporize 100% of the precursor and transport it into the deposition chamber before it begins to decompose. This type of liquid delivery systems has been used for the deposition of metals and especially metal oxides.

Aerosol-assisted (AA) CVD also involves dissolution of the precursor in a suitable solvent, but the solution is dis-

[\*] Dr. C. Vahlas, Dr. F. Senocq, L. Aloui  
Centre Interuniv. de Recherche et d'Ingénierie des Matériaux  
(CIRIMAT CNRS), ENSIACET  
118 route de Narbonne, 31077 Toulouse cedex 4 (France)  
E-mail: Constantin.Vahlas@ensiacet.fr

Prof. B. Caussat  
Laboratoire de Génie Chimique (LGC CNRS-INPT)  
5 rue Paulin Talabot, BP1301, 31106 Toulouse Cedex 1 (France)

Prof. W. L. Gladfelter, T. Moersch  
Chemistry Department, University of Minnesota  
207 Pleasant St. SE, Minneapolis, MN 55455 (USA)

[\*\*] We are indebted to D. Sadowski for technical support, to D. Toro, Ch. Sarantopoulos, and P. Venios for experimental work. This project was supported by CNRS-NSF grant #14562 between CIRIMAT and the Chemistry Department of the University of Minnesota, by grants from the National Science Foundation (INT-0233328 and CHE-03159540), and by a Bonus Qualité Recherche grant from the National Polytechnic Institute of Toulouse.

persed by formation of an aerosol.<sup>[6,7]</sup> Ideally, the droplets are completely volatilized before they hit the substrate. In both the AA and liquid-precursor delivery systems large amounts of solvent are carried into the CVD reactor, which can increase impurity incorporation into the film. A variation of the solution approach has recently appeared in which the precursor is placed in an inert solvent that has a lower vapor pressure than the precursor itself. Thus, a typical liquid bubbler can be used.<sup>[8]</sup> An alternative route deals with a solid-precursor delivery system that does not involve adding any solvent.<sup>[9]</sup> Following this method the solid precursor is directly transported to a flash evaporator and, from this location, the precursor vapor is transported into the reaction chamber. Small inert beads are added to the solid precursor to improve the reliability of the particle transport.

The present paper further develops and details first results on the design, construction and testing of a reliable solid precursor delivery system for CVD reactors based on fluidized-bed (FB) technology that have been presented in the literature.<sup>[10]</sup> FB systems are commonly used for improving the transport phenomena in gas-particle systems.<sup>[11]</sup> In the present case, the FB is composed of either pure precursor or precursor mixed with inert powder. The bed is heated at the sublimation temperature and the fluidization gas is enriched with the precursor vapor. This gas phase enters the CVD reactor which is positioned at the exit of the FB reactor. Sublimation of tris(pentan-2,4-dionato)aluminum,  $[Al(acac)_3]$ , is used as a model system. A model is presented that compares the performance of the FB system to that of a fixed-bed delivery system. The characteristics of the powders and their ability to be fluidized will be presented. Finally, the FB delivery system will be used for the MOCVD of alumina coatings on titanium alloys for their protection against oxidation at moderate temperature.

## 2. Theoretical Base

The following model has been established in order to describe properly the flux of precursor at the exit of the sublimator process, and the ability of different vessel designs to deliver precursor vapors. Steady-state conditions and thermal equilibrium (gas, bubbler, precursor bed at the same temperature) are assumed in this model. Figure 1 schematically presents a sublimator with the parameters which are considered in the model. There is a differential element of volume  $dV$  of carrier gas at position  $y$ , flowing from the top through a bed of precursor powder with height  $h$  and radius  $r$ , placed on a porous inert barrier, e.g., a sintered glass.

The molar flux of precursor  $F_{Pr}$  per surface area entering the elemental volume  $dV$  can be written as Equation 1.

$$F_{Pr} = a(C_T - C_y) \quad (1)$$

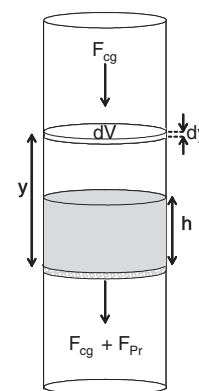


Fig. 1. Schematic drawing of the fixed-bed sublimator.

$C_T$  is the molar concentration of saturated precursor vapor at  $T$ ,  $C_y$  is effective concentration in  $dV$  at position  $y$ , and  $a$  is a mass transfer coefficient.  $F_{Pr}$  can also be written as Equation 2.

$$F_{Pr} = (P_T - P_y)a/RT \quad (2)$$

$P_T$  is the saturated vapor pressure of precursor at  $T$ ,  $P_y$  is the effective vapor pressure in  $dV$  at position  $y$ . If  $n$  is the number of precursor moles entering  $dV$ , then this can be further written as Equation 3, where  $ds = 2\pi r dy$ .

$$F_{Pr} = d^2n/dsdt \quad (3)$$

Pushed down by the carrier gas flow rate,  $dV$  goes through the bed at a velocity  $v = dy/dt$ . Replacing in Equation 3 yields  $F_{Pr} = (d^2n/dy^2)v/2\pi r$ . Taking into account Equation 2, this expression yields Equation 4.

$$d^2n = [(2\pi r a)/(vRT)](P_T - P_y)dy^2 \quad (4)$$

Considering the ideal gas law and after integration, Equation 4 yields Equation 5.

$$P_y = P_T[1 - \exp(-a y/vr)] \quad (5)$$

Since  $v = F_{cg}/\pi r^2$ , where  $F_{cg}$  is the carrier gas volumic flow rate, then this becomes Equation 6.

$$P_y = P_T[1 - \exp(-a\pi r y/F_{cg})] \quad (6)$$

After having crossed the precursor bed through the height  $h$ , Equation 6 can be written as Equation 7.

$$P_{Pr} = P_T[1 - \exp(-\beta Q/F_{cg})] \quad (7)$$

$P_{Pr}$  is the precursor vapor pressure at the exit of the bed,  $\beta$  is a mass transfer coefficient, and  $Q$  is the mass of the precursor. The steady state assumption allows writing  $F_{Pr}/F_{cg} = P_{Pr}/P_{cg}$ , where  $P_{cg}$  is the pressure of the carrier

gas, which equals  $P_{cg} = P_{tot} - P_{pr}$ . Consequently, Equation 7 can be written as Equation 8.

$$F_{pr} = F_{cg} P_T [1 - \exp(-\beta Q / F_{cg})] / [P_{tot} - P_T (1 - \exp(-\beta Q / F_{cg}))] \quad (8)$$

In the frequent case of  $P_{tot} \gg P_T$ , Equation 8 can be simplified as Equation 9.

$$F_{pr} = (F_{cg} P_T / P_{tot}) [1 - \exp(-\beta Q / F_{cg})] \quad (9)$$

In this final equation,  $\beta$  has the dimension of a mass transfer coefficient, and it is correlated with the nature of the precursor, its specific surface area (i.e., the distribution of the grain size and porosity), the temperature, and the bubbler efficiency. From Equation 9, the precursor flow rate is related only with the experimental conditions (temperature, carrier gas flow rate, operating pressure, quantity of precursor), and with the  $\beta$  coefficient, the only required external information being the relation of precursor vapor pressure vs. temperature. For the same precursor batch, higher values of  $\beta$  lead to more efficient bubbler operation and, ultimately, higher precursor flow rates ( $F_{pr}$ ).  $\beta$  is also temperature dependent and has to be determined experimentally for each temperature. This can be done by measuring the mass loss in a bubbler operated at fixed  $T$  and  $P_{tot}$  (and, for the ease of experimentation, the same initial amount of precursor) for different carrier gas flow rates. It is worth noting that the increase of the precursor flow rate cannot be obtained from the increase of the carrier gas flow rate because the mathematical limit of the precursor flow rate at fixed  $P_{tot}$  and  $T$  is given by  $F_{max} = \beta Q P_T / P_{tot}$ .  $F_{pr}$  can be increased by decreasing  $P_{tot}$  and/or by increasing the sublimation temperature. However, both directions may be technologically limited. By increasing the amount of precursor in the bubbler, one can increase the precursor flow to the upper limit corresponding to the saturation of the gas phase in precursor vapor (Eq. 10).

$$F_{max} = F_{cg} P_T / P_{tot} \quad (10)$$

Increasing the amount of the precursor in the sublimator is a suitable solution when i) the volume of the bubbler is not a limitation in the process, ii) the cost of the precursor (due to the large amounts used) is acceptable, and iii) the thermal stability of the precursor (related with the use of large quantities) is compatible with long term operation. Although all these conditions are fulfilled for  $[\text{Al}(\text{acac})_3]$ , they are not necessarily satisfied for other precursors. In that case, the only solution is the development of improved concepts of the evaporator in order to increase the value of  $\beta$ , and consequently the precursor flow rate.

For a given set of experimental conditions, the model accurately describes the initial precursor flow rate as well as its evolution throughout the duration of the experiment. This point is important in the case of precursors with high

vapor pressure or when a high flow rate of the precursor is required. The latter case is illustrated by the work of Duminica et al. on the MOCVD of iron from ferrocene,  $\text{Fe}(\text{C}_5\text{H}_5)_2$ .<sup>[12,13]</sup> The authors used a conventional saturator ( $\beta = 800 \text{ cm}^3 \text{ g}^{-1} \text{ min}^{-1}$ ) under atmospheric pressure. Figure 2 presents the calculated flow rates of ferrocene as a function of operating time for a value of the saturated vapor pressure equal to 344 Pa, obtained by maintaining the sublimator at 373K. Results are presented for different initial quantities of  $\text{Fe}(\text{C}_5\text{H}_5)_2$  in the sublimator. Under these conditions, an initial charge of 8 g of  $\text{Fe}(\text{C}_5\text{H}_5)_2$  produces a constant precursor flow during a one hour run.

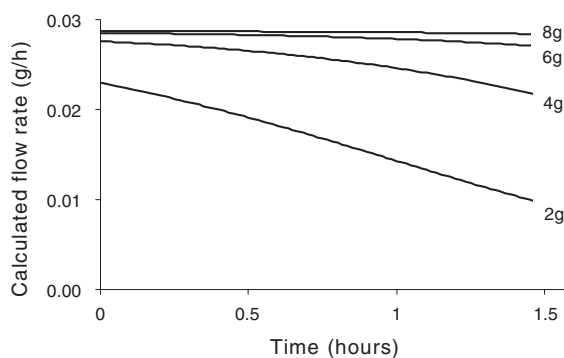


Fig. 2. Calculated  $\text{Fe}(\text{C}_5\text{H}_5)_2$  flow rates (in  $\text{g h}^{-1}$ ) versus time (hours) at 373K,  $\text{N}_2$   $F_{cg} = 1000 \text{ scm}$ , under atmospheric pressure ( $P_T = 344 \text{ Pa}$ ) for various initial loads of the precursor in the sublimator.

However, the  $\text{Fe}(\text{C}_5\text{H}_5)_2$  flow rate under these conditions ( $0.03 \text{ g h}^{-1}$ ) is relatively low. To increase this value the sublimator temperature can be increased to 423K, which is compatible with the high thermal stability of this compound. Figure 3 illustrates the calculated flow rates of ferrocene as a function of operating time and of the initial sublimator charge for a value of the saturated vapor pressure equal to 5630 Pa at 423K. Under these conditions  $\beta$  equals  $400 \text{ cm}^3 \text{ g}^{-1} \text{ min}^{-1}$ . Although the precursor flow rate is 16 times greater, more than 35 g are necessary to ensure 1 h of steady operation.

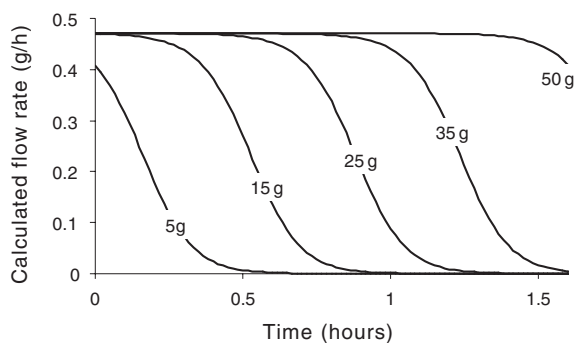


Fig. 3. Calculated  $\text{Fe}(\text{C}_5\text{H}_5)_2$  flow rates (in  $\text{g h}^{-1}$ ) versus time (hours) at 423K,  $\text{N}_2$   $F_{cg} = 1000 \text{ scm}$ , under atmospheric pressure ( $P_T = 5630 \text{ Pa}$ ) according to various initial loads.

The present model is not a fully descriptive one. Applied to the fluidized bed it deals neither with heat and mass transfer phenomena nor with fluid mechanics, nor with the evolution of particle size vs. time, etc. as is reviewed in the literature.<sup>[14]</sup> Although potentially highly accurate and predictive, such a calculation requires appropriate data and would be time consuming. However, despite its simplicity, the present model can be used to describe accurately the evaporation rate of a CVD precursor in a saturator (provided its Clausius-Clapeyron law is known) and to guide the choice of operating conditions to optimize the CVD process.

### 3. Reactor Design

Figure 4 presents the schematic of the conventional, glass sublimator that was used for fixed-bed experiments. Pure nitrogen, preheated to the sublimation temperature, was used as the carrier gas. At the exit, the sublimator was connected to a liquid nitrogen-cooled trap by a gas line maintained above sublimation temperature to avoid any premature condensation. The operating temperature was fixed at 393K using a heating blanket.

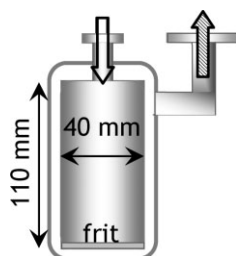


Fig. 4. Schematic of the conventional glass sublimator that was used for fixed-bed experiments.

Figure 5 presents the schematic of the FB sublimator, designed following the classic concepts of fluidization engineering.<sup>[15]</sup> It is composed of a stainless steel tube, 50 mm in internal diameter and 500 mm in height. At its two extremities it is connected with conical metallic pieces ensuring the connection with the inlet and outlet gas lines. A metallic grid is positioned at its bottom to maintain the bed of particles at rest and to distribute the fluidization gas evenly. Elutriation of fines and transport of powders to the CVD reactor is prevented by using chicanes and an appropriate filter near the tube exit. The FB sublimator is fed with pure nitrogen whose flow rate is monitored by two mass flow controllers (MFCs) (Brooks) in the range 500 sccm and 10000 sccm. MFCs are mounted in parallel to ensure fine tuning of gas flow rate over a wide operating range. The temperature of the set-up from the exit of the flow meters to the entrance of the CVD reactor is regulated through the use of heating ribbons for the connecting tubes and five collars for the FB. Each one is monitored by a PID controller and a thermo-

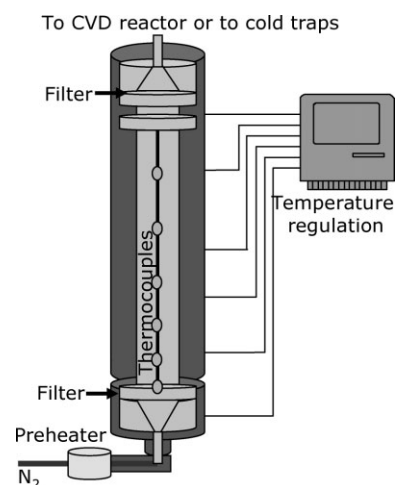


Fig. 5. Schematic of the FB sublimator.

couple. The entire heated zone is thermally insulated. Six thermocouples are positioned inside the FB on its central axis to monitor temperature in and above the sublimation zone. Pressure drop across the bed is monitored by a differential pressure transducer (Druck LPX 5480) operating in the range 0–10 000 Pa. Output from the six thermocouples and from the differential pressure transducer is collected through individual data acquisition modules (Dataforth 5B47K) which are connected to a DaisyLab running PC through an analog signal conditioning input board (IOtech DBK207) and a data PCI board (IOtech DaqBoard/2005).

The bed is heated at the sublimation temperature and the fluidization gas is enriched with the gaseous precursor. The FB sublimator is connected at its exit either to a cold trap system or to a CVD reactor. The cold trap system is composed of two glass traps mounted in series. During operation they are maintained at 223K by immersion in liquid nitrogen-cooled ethanol baths. A by-pass system prevents the gas flow from crossing the traps during the heating and cooling stages of the process. Experiments were performed under the same conditions at various carrier gas flow rates. For each experiment, trapping of condensed precursor lasted 30 min. After each run, the traps were removed from the line and acetone was used to extract the precursor. Following evaporation of the acetone, the solid precursor was weighed. Preliminary CVD experiments were performed in a resistively heated reactor, composed of a vertical quartz tube of 25 mm ID and 300 mm in height, closed at its two extremities by metallic flanges connected to the inlet and exit tubes. Samples were maintained welded on a regulation thermocouple, which is positioned close to the sample along the central axis of the reactor.

### 4. Materials Choice

Sublimation of  $[\text{Al}(\text{acac})_3]$  is used as a model system. This is a common, solid precursor for the CVD of alumi-

na<sup>[16]</sup> with a low saturated vapor pressure provided by the expression  $\log P(\text{kPa}) = 3.44 - 2359/T(\text{K})$ .<sup>[17]</sup> A sublimation temperature of 393K, corresponding to a vapor pressure of 2.7 Pa, was adopted in the present report. As-received  $[\text{Al}(\text{acac})_3]$  powder (Acros Organics) has a particle size distribution with a volume mean value of 30  $\mu\text{m}$  and with 10% of the particles less than 3  $\mu\text{m}$ . The aspect ratio, specific surface area, and porosity of particles were determined to be 0.93, 1.21  $\text{m}^2 \text{g}^{-1}$ , and 0.06, respectively. Taking into account a bulk density of 1.27  $\text{g cm}^{-3}$ , the density of  $[\text{Al}(\text{acac})_3]$  grains equals 1.19  $\text{g cm}^{-3}$ . Based on these measurements, this powder belongs to Geldart's group C;<sup>[18]</sup> therefore, it is expected to be cohesive and a priori not fluidizable. The diagram of Figure 6 presents the differential pressure  $\Delta P$  vs. gas velocity for three runs at decreasing flow rate across a bed composed of pure  $[\text{Al}(\text{acac})_3]$ . Data were obtained at 393K for a ratio of the height of the bed

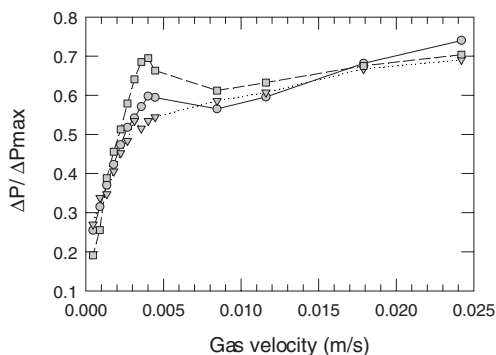


Fig. 6. Differential pressure vs. gas velocity for three runs at decreasing flow rates across a bed composed of pure  $[\text{Al}(\text{acac})_3]$  with  $H/D = 3$ , maintained at 393K.

at rest over the diameter of the column  $H/D$  equal to 3. Values of  $\Delta P$  are normalized with regard to  $\Delta P_{\text{max}}$ ; i.e., the differential pressure calculated from the bed weight and corresponding to optimum fluidization. At low flow rates there is a linear increase of  $\Delta P$  with, however, a discrepancy from one run to another. Such a discrepancy is particularly noticeable in the minimum fluidization zone, i.e., around 0.003 and 0.008  $\text{m s}^{-1}$ . Moreover,  $\Delta P$  does not remain constant and equal to  $\Delta P_{\text{max}}$  in the fluidization regime. In addition, the mean value of  $\Delta P$  above  $U_{\text{mf}}$  is far lower than  $\Delta P_{\text{max}}$ , and finally, important differences appear between the increasing and the decreasing curves (not shown in the diagram). Similar behavior is obtained in other operating conditions, namely for  $D$  equal to 24 mm and for  $H/D$  ratios between 2 and 5. It thus appears that the fluidization quality of pure  $[\text{Al}(\text{acac})_3]$  is poor due to strong interparticle forces, which are mainly related to the low mean diameter and density of these powders.

In order to reach maximum thermal and mass transfer inside the bed, and consequently to operate in reproducible conditions ensuring maximum sublimation, it is necessary to optimize the hydrodynamic behavior of the bed. In view

of the above results, it is concluded that addition of an inert medium with adequate fluidization behavior is necessary for the efficient operation of the FB sublimator. This point should be considered as an advantage rather than a constraint, because the design of the reactor and its operating conditions can be now based on appropriately selected inert media for the fluidization, thus providing extended applicability of the reactor to a series of molecular or inorganic precursors. Moreover, it appears that the quantity of the precursor involved in each run is not related to that of the bed, allowing for economic and environmentally compatible handling of the precursors.

In addition to high fluidization quality, the fluidization support must be physically and chemically inert, non toxic, attrition resistant, inexpensive, and have a melting temperature much greater than the fluidization temperature. In this context, two fluidization supports have been tested, both belonging to Geldart's group B: alumina  $\text{Al}_2\text{O}_3$  and silica  $\text{SiO}_2$  powders. The grain density of the alumina (Balkowski) and silica (Humeau) powders that were used in the present experiments are 3.96  $\text{g cm}^{-3}$  and 2.65  $\text{g cm}^{-3}$ , respectively. Prior to their use, as-received powders were sieved resulting in particle size between 128  $\mu\text{m}$  and 353  $\mu\text{m}$  with a mean value of 226  $\mu\text{m}$  in volume for alumina, and between 144  $\mu\text{m}$  and 293  $\mu\text{m}$  with a mean value of 213  $\mu\text{m}$  in volume for silica. The ability to use two different, easily fluidizable supports provides flexibility in the choice of the minimum fluidization velocity ( $U_{\text{mf}}$ ) for a given flow rate of the fluidizing gas. An example of the fluidization behavior of different mixtures of the precursor with the inert support is presented in Figure 7 for operation at ambient temperature. Pressure drop as a function of gas velocity is reported for four mixtures of  $[\text{Al}(\text{acac})_3]$  with alu-

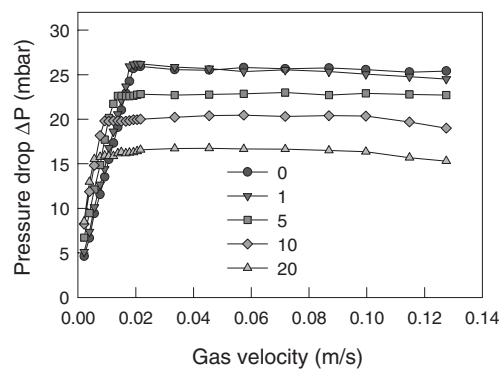


Fig. 7. Pressure drop as a function of gas velocity at decreasing flow rate and of the percentage of  $[\text{Al}(\text{acac})_3]$  for an alumina bed with  $H/D$  ratio of 3, measured at ambient temperature.

mina, namely 1 wt.-%, 5 wt.-%, 10 wt.-%, and 20 wt.-%, together with the corresponding behavior of a bed composed of pure alumina powder. Fluidization is observed for all concentrations for gas velocities up to  $4U_{\text{mf}}$ . For beds with the two highest  $[\text{Al}(\text{acac})_3]$  content, the pressure drop

starts decreasing above a gas velocity of  $0.1 \text{ m s}^{-1}$ . This is attributed to the initiation of elutriation of the finest  $[\text{Al}(\text{acac})_3]$  particles in these conditions. Behavior of the bed in all other investigated conditions corresponds to that of pure alumina. Fluidization at 393K yields similar results.

## 5. Sublimation Results

All experiments have been conducted under atmospheric pressure. Figure 8 presents the flow rate of the precursor vs.  $\text{N}_2$  flow rate generated in the fixed-bed sublimator, maintained at 393K. The dots on the diagram correspond to experimental results obtained with a bed of 10.5 g of

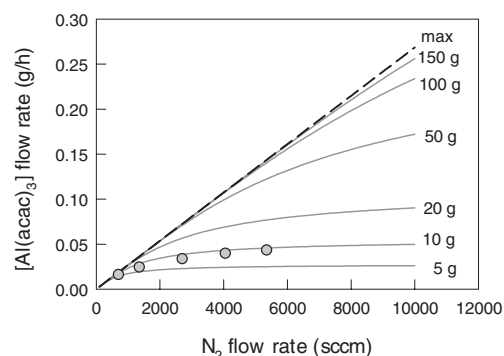


Fig. 8. Flow rate of  $[\text{Al}(\text{acac})_3]$  as a function of nitrogen flow rate in the fixed-bed sublimator. Experimental results (circles), theoretical upper limit of the flow rate (dashed line), and estimated flow rates for various quantities of the precursor in the sublimator (grey lines).

$[\text{Al}(\text{acac})_3]$ . The straight dashed line corresponds to the theoretical maximum efficiency of the sublimator following Equation 10. Application of Equation 9 provides, in this case, a value of  $\beta$  equal to  $205 \text{ cm}^3 \text{ g}^{-1} \text{ min}^{-1}$ . Conversely, by introducing this value into Equation 9,  $F_{\text{pr}}$  can be estimated under the same conditions but for various values of  $Q$ . The results are illustrated in Figure 8 by the different grey lines. It is concluded that for sublimation conditions involving such a fixed bed, a large quantity of  $[\text{Al}(\text{acac})_3]$ , namely 150 g, is necessary to approach the maximum efficiency of the process.

From Figure 8, a nitrogen flow rate of 4000 sccm produces an initial flow rate of  $[\text{Al}(\text{acac})_3]$  of  $0.0398 \text{ g h}^{-1}$ . According to the model presented herein, this value becomes  $0.0387 \text{ g h}^{-1}$  after 10 h and  $0.0376 \text{ g h}^{-1}$  after 20 h. (variation  $\approx -5\%$ ). If the initial quantity of the precursor is increased to 30 g, the initial  $[\text{Al}(\text{acac})_3]$  flow rate will be  $0.0753 \text{ g h}^{-1}$ , and it will decrease to  $0.0737 \text{ g h}^{-1}$  after 20h ( $\approx -2\%$ ). It can be concluded that, at least for laboratory time scales, the  $[\text{Al}(\text{acac})_3]$  flow rate is in these conditions nearly constant. This is due to its low saturated vapor pressure providing very low evaporation rate.

Figure 9 presents experimental results of the  $[\text{Al}(\text{acac})_3]$  flow rate as a function of nitrogen flow rate in the FB reac-

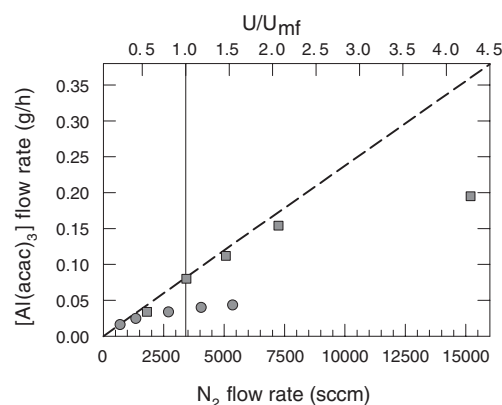


Fig. 9. Experimental results of  $[\text{Al}(\text{acac})_3]$  flow rate as a function of nitrogen flow rate, and of the corresponding gas velocity  $U$ , reported to the minimum fluidization velocity  $U_{\text{mf}}$ . Sublimation in the FB (squares) and in the fixed bed (circles). Dashed line corresponds to the theoretical upper limit of the flow rate under the adopted operating conditions.

tor. The bed temperature was maintained at 393 K, as in fixed-bed conditions.  $H/D$  in this case was equal to 3, and the bed consisted of 720 g of silica powder and 10.5 g (1.46 wt.-%) of  $[\text{Al}(\text{acac})_3]$ . Data on the fixed bed results from Figure 8 are also included on Figure 9 for comparison. Sublimation in FB yields considerably higher  $[\text{Al}(\text{acac})_3]$  flow rates than in fixed bed under similar conditions. Moreover, sublimation efficiency is strongly improved so as to approach the theoretical upper limit of the flow rate, except for the last point at 15000 sccm corresponding to  $U/U_{\text{mf}} = 4$ . The lower value observed for this point is an artifact due to the reduced efficiency of the trapping system operating at these high flow rate conditions. A significant portion of the precursor was transported through the traps to the exhaust tube and was not considered in the determination of the transported mass of the precursor. It is worth noting that carrier gas flow rates up to 20000 sccm and corresponding high precursors flow rates are compatible with numerous industry implemented processes such as the surface treatment of steels and glass in production lines. Data obtained at the lowest nitrogen flow rate; i.e., at 1800 sccm ( $U/U_{\text{mf}} = 0.5$ ), correspond to sublimation under fixed bed conditions. Considering the three intermediate points ( $U/U_{\text{mf}} = 1, 1.5, \text{ and } 2$ ) the value of  $\beta$  was calculated to be  $1450 \text{ cm}^3 \text{ g}^{-1} \text{ min}^{-1}$ , to be compared with  $205 \text{ cm}^3 \text{ g}^{-1} \text{ min}^{-1}$  for the fixed bed. This value is decreased to  $270 \text{ cm}^3 \text{ g}^{-1} \text{ min}^{-1}$  for  $U/U_{\text{mf}} = 0.5$ ; i.e., the performance of the present apparatus operating in fixed bed conditions becomes comparable, though higher, with that of the conventional fixed bed sublimator.

## 6. CVD of Alumina

Preliminary experiments of the MOCVD of alumina were performed under the sublimation conditions  $T = 393\text{K}$ ,  $U/U_{\text{mf}} = 2$ ,  $H/D = 3$ , and 1.46 wt.-% of  $[\text{Al}(\text{acac})_3]$

in silica powder. These conditions ensure the feeding of the CVD reactor with 0.19 sccm of  $[\text{Al}(\text{acac})_3]$ . An additional gas line was used to feed the CVD reactor with 100 sccm of oxygen bubbling through a  $\text{H}_2\text{O}$  bath maintained at 343K. Depositions were performed on thermally grown silica and on commercial Ti6242 titanium alloy coupons. Ti6242 is used in helicopter turbine components submitted to moderate stresses. The role of alumina coating is to improve its surface properties in high temperature oxidation and corrosion conditions. The deposition temperature was fixed at 853K in order to maintain the microstructural integrity of the Ti6242 alloy. 300 nm thick amorphous alumina films were deposited in 3 h runs. Films are smooth and do not contain any heteroatoms, namely carbon. Coated coupons were subjected to thermogravimetric analysis in dry air. At 873K; i.e., at the upper limit of service temperature for this material, oxidation kinetics were two orders of magnitude lower than those of bare alloy. These preliminary results show promise for the deposition of alumina coatings by the present process on different parts of turbines for aeronautics and energy applications.

## 7. Conclusions

We successfully designed, constructed, and tested a fluidized bed precursor delivery system to overcome the mass and heat transport problems encountered in a fixed-bed system. To achieve ideal fluidization behavior, a combination of solid precursor (minor component) and inert particles such as alumina or silica (major component) were charged to the vessel. Using  $[\text{Al}(\text{acac})_3]$  as a test precursor and operating a 423K, the rate of mass transport was measured as a function of carrier-gas flow rate. The precursor and carrier gas mixture were directed into a CVD reactor where the flow was combined with a source of water vapor and oxygen to deposit amorphous  $\text{Al}_2\text{O}_3$  films on wafers of a Ti6242 alloy.

A model of a solid-precursor delivery system was developed to quantify the relationship between operating conditions and gas-phase precursor flow rate. For a given vessel temperature, the flux of mass transported depended on the carrier-gas flow rate, the amount of precursor present in the vessel, the ratio of the precursor vapor pressure to the total pressure, and a mass transport coefficient ( $\beta$ ). The value of  $\beta$  was dependent upon the surface area of the precursor, the particle size distribution, and the bubbler efficiency. When operating at carrier-gas flow rates above the minimum value required to fluidize the bed, the precursor flow rate (and the value of  $\beta$ ) for the FB delivery system significantly exceeded the performance of the fixed-bed system.

Received: April 24, 2006

Revised: July 24, 2006

- [1] M. K. Lee, D. S. Wu, H. H. Tung, *Appl. Phys. Lett.* **1987**, *50*, 1805.
- [2] B. C. Hendrix, T. H. Baum, D. D. Christos, J. F. Roeder, *US Patent US6340386*, **2002**.
- [3] T. H. Baum, *US Patent US6344079*, **2002**.
- [4] G. Bhandari, T. H. Baum, *US Patent US6099653*, **2000**.
- [5] B. Zheng, E. T. Eisenbraun, J. Liu, A. E. Kaloyeros, *Appl. Phys. Lett.* **1992**, *61*, 2175.
- [6] C. Xu, M. J. Hampden-Smith, T. T. Kodas, *Adv. Mater.* **1994**, *6*, 746.
- [7] C. Xu, M. J. Hampden-Smith, T. T. Kodas, *Chem. Mater.* **1995**, *7*, 1539.
- [8] F. R. McFeely, D. A. Neumayer, J. J. Yurkas, *US Patent US6984415*, **2006**.
- [9] I. S. Chuprakov, J. D. Martin, K. H. Dahmen, *J. Phys. IV* **1999**, *9*, 901.
- [10] C. Vahlas, B. Caussat, F. Senocq, W. L. Gladfelter, C. Sarantopoulos, D. Toro, T. Moersch, *Electrochem. Soc. Proc.* **2005**, *2005-09*, 221.
- [11] C. K. Gupta, D. Sathiyamoorthy, *Fluid Bed Technology in Materials Processing*, CRC Press, Boca Raton, FL **1999**.
- [12] F. D. Duminica, *Ph.D. Thesis*, National Polytechnic Institute, Toulouse **2004**.
- [13] F. D. Duminica, F. Maury, F. Senocq, *Récents Progrès en Génie des Procédés*, Lavoisier, Paris **2005**, P-2.
- [14] C. Vahlas, B. Caussat, P. Serp, G. N. Angelopoulos, *Mater. Sci. Eng. R* **2006**, *53*, 1.
- [15] D. Kunii, O. Levenspiel, *Fluidization Engineering*, Butterworth-Heinemann, Newton, MA **1991**.
- [16] M. P. Singh, S. A. Shivashankar, *Surf. Coat. Technol.* **2002**, *161*, 135.
- [17] R. Theghil, D. Ferro, L. Bencivenni, M. Pelino, *Thermochim. Acta.* **1981**, *44*, 213.
- [18] D. Geldart, *Powder Technol.* **1973**, *7*, 285.